CrossMark

Effects of microRNA-21 on Nerve Cell Regeneration and Neural Function Recovery in Diabetes Mellitus Combined with Cerebral Infarction Rats by Targeting PDCD4

Yun-Bao Guo[1] · Tie-Feng Ji[2] · Hong-Wei Zhou[2] · Jin-Lu Yu[1]

Abstract We aimed to determine the effect and mechanism of microRNA-21 (miR-21) on nerve cell regeneration and nerve functional recovery in diabetes mellitus combined with cerebral infarction (DM + CI) rats by targeting PDCD4. A total of 125 male Wistar rats were selected for DM + CI rat model construction and assigned into the blank, miR-21 mimics, mimics control, miR-21 inhibitor, inhibitor control, miR-21 inhibitor + si-PDCD4 and si-PDCD4 groups. And, 20 healthy rats were selected for the normal group. Triphenylterazolium chloride (TTC) staining and HE staining were used for determination of the area of CI and pathological changes, respectively. Behaviors of rats in the eight groups were determined by forelimb placement test and balance beam walking test. Immunohistochemical staining, double immunofluorescence staining assay, Western blotting, and qRT-PCR were used to detect expressions of miR-21, PDCD4, HNA, Nestin, NeuN, β-III-Tub, PTEN, FasL, and GFAP. DNA laddering and TUNEL staining was used for cell apoptosis. TTC and HE staining confirmed that 87.5% rats were induced into CI + DM models successfully. Results of forelimb placement test and balance beam walking test showed that miR-21 mimics, and si-PCDC4 improved the nerve defect of model rats. Comparing with the blank group at the same time, rats in the miR-21 inhibitor group displayed significant decrease in the

forelimb placement test score, significant increase in the balance beam walking test score, and exacerbation of nerve defect, while rats in the miR-21 mimics and si-PCDC4 groups displayed significant increase in forelimb placement test score and significant decrease in the balance beam walking test score and improvement of nerve defect situation. The HNA, Nestin, and PDCD4 expressions were decreased and the NeuN, β-III-Tub, and GFAP expressions were increased in the miR-21 mimics and si-PDCD4 groups comparing with the blank group. The results of miR-21 inhibitor group were on the contrary. In comparison to the blank group, the miR-21 mimics group and the si-PDCD4 had lower miR-21 expressions and higher expressions of PDCD4, PTEN, and FasL, while the miR-21 inhibitor group was in the opposite trend. The results of qRT-PCR were the same with Western blotting. The expressions of fluorescence in other groups were higher than the normal group; compared with the blank group, the miR-21 mimics group and the si-PDCD4 group had lower fluorescence expression and DNA ladder. However, the fluorescence expressions and DNA ladder of miR-21 inhibitor group increased markedly in contrast with the blank group. Comparing with the blank group, BrdU$^+$/DEX$^+$ fluorescence intensity significantly enhanced in the miR-21 mimics and si-PDCD4 groups and significantly reduced in the miR-21 inhibitor group. And, comparing with the blank group, in the miR-21 mimics group, the signal strength of luciferase carrying the wild-type PDCD4 was reduced by 25%. The present studies demonstrated that miR-21 could promote the nerve cell regeneration, suppress apoptosis of nerve cells in DM + CI rats and improves the nerve defect situation of DM + CI rats by inhibiting PDCD4.

✉ Jin-Lu Yu
jinlu_yu@hotmail.com

1 Department of Neurosurgery, The First Hospital of Jilin University, No. 71, Xinmin Road, Chaoyang District, Changchun 130021, Jilin Province, People's Republic of China

2 Department of Radiology, The First Hospital of Jilin University, No. 71, Xinmin Road, Chaoyang District, Changchun 130021, People's Republic of China

Introduction

Diabetes mellitus (DM), a metabolic disease, is characterized by high glucose or blood sugar levels, leading to worsening or severe insulin resistance [1]. As a heterogeneous disorder, DM has two main types, namely, type 1 DM (T1DM) and T2DM: the T1DM usually occurs in childhood and T2DM is deemed as the most common form of DM with an increasing prevalence worldwide [2, 3]. Previous evidence reveals that DM increases the risk of heart disease, stroke, and some microvascular complications, including blindness, peripheral neuropathy, and renal failure [2]. Cerebral infarction (CI) is mainly due to a lack of blood supply in brain tissue including neural cells, glial cells, and vascular necrosis, and diabetes is a risk factor for CI [4]. The incidence of DM patients with CI increases and the proposed pathogenesis include metabolic injury to nerve fibers, nervous damage, sorbitol accumulation, fatty acid alterations, protein glycosylation, neurotrophic growth factor reduction, and autoimmune damage [5]. Conventional medical treatment of DM only partially achieves adequate glycemic control and a reduction in cardiovascular risk and lack of prevention of stroke [3]. Besides, conventional therapeutic strategies for CI include thrombolytic therapy, antithrombotic therapy, and prevention of neuronal dysfunction and death [6]. Nowadays, there have been great progresses in gene targeting therapy which may be a new method for clinical DM + CI therapy.

MicroRNAs, a class of non-coding small RNAs, bind the 3′UTR of target genes and thereby repress translation of target genes and/or induce degradation of target gene mRNA [7]. The microRNA-21 (miR-21) is one of the miRNA family, which is associated with poor survival and therapeutic outcome in malignant cancer [8]. Programmed cell death protein 4 (PDCD4) is associated with apoptosis and reduction of PDCD4 could protect cells by inhibiting apoptosis [9]. Substantial data indicate that PDCD4 is consistently down-regulated in human cancer and cancer cell lines [10]. It has been reported that miR-21 directly targets the 3′ UTR region of PDCD4 and downregulates its expression [11] and as one of the most important target genes of miR-21, PDCD4 is also associated with antiapoptosis effect of miR-21 [9]. Previous studies reported the targeted effects of miR-21 on PDCD4 in prostatic cancer and colorectal cancer. However, the effect of miR-21-targeted PDCD4 on nerve cell regeneration and nerve functional recovery in DM + CI rats has not been reported. Thus, in this study, the role of miR-21 on nerve cell regeneration and nerve functional recovery in DM + CI rats by targeting PDCD4 was proposed and the basis evidences of research of miR-21 targeted gene therapy for DM + CI was provided.

Methods and Materials

Subjects

Healthy adult male Wistar rats ($n = 145$), aged 8 weeks and weighted 220 ± 25 g, were purchased from Institute of Zoology, Chinese academy of sciences. All the rats were clean level and divided into two groups randomly. Both of the two groups of rats were adopted in individual cages and healthy diet under 25 ± 1 °C and 50% humidity. All the rats were treated according to national regulations on animal experiment requirements and approved by the association of The First Hospital of Jilin University animal ethics. Animals were treated with as much kindness as possible to reduce their pain.

Establishment of DM + CI Rat Model

The rat models were established through two times of administration. Experimental rats ($n = 125$) were intraperitoneally injected with 100 mg/kg alloxan for two consecutive days. The fasting blood glucose of the rats in 72 h after the last injection was detected by glucose oxidase method. The DM model rats were successfully established when fasting blood glucose value reaches to 16.7 mmol/L or more. After being fed with high-fat diet for five consecutive weeks, the DM rats were anesthetized by 20% urethane through intraperitoneal injection. Suture method was used to make middle cerebral artery occlusion (MCAO) models. Room temperature was maintained at 24 ± 1 °C. The anesthetic rats were placed in the dorsal position and fixed on the operating table. The incision was made in the neck midline, and the right common carotid artery (CCA), external carotid artery (ECA), and internal carotid artery (ICA) were separated and exposed, followed by ligation of the side of proximal part of right CCA and the root of ECA. The upper wall of ICA was pierced by a needle from the distal end of ICA, and a nylon line (0.25 mm diameter) was inserted into CCA (from ICA to the start of artery). The insertion was stopped and the suture was fixed when the resistance appeared, followed by the suture of incision. The models were established successfully when rats walk to the left rotation or had paralysis in left limb after waking up. Successful model rats were contained into the following experiment; otherwise, the failed rat model was abandoned.

Plasmid Construction and Grouping

The normal group contains 20 healthy rats (healthy control). Rat models ($n = 105$) were randomly selected and divided into the following seven groups ($n = 15$): the blank group (without transfection), the miR-21 mimics group (transiently transfected with miR-21 mimics), the mimics control group (transfected with negative control of miR-21 mimics), the miR-21 inhibitor group (transiently transfected with miR-21

inhibitor), the inhibitor control group (transiently transfected with negative control of miR-21 inhibitor), the miR-21 inhibitor + si-PDCD4 group (transiently transfected with miR-21 inhibitor + PDCD4 siRNA), and the si-PDCD4 group (transfected with PDCD4 siRNA). PCDC4 was silenced by siRNA. Three days after rat models were established, plasmid and corresponding inhibitor was injected according to the groups in the lateral ventricle once a day for seven consecutive days. The rats were fed for 28 days during the same period after injection and put to death to obtain their brain tissue for animal experiments.

Triphenyltetrazolium Chloride Staining

After model establishment, 20% urethane was intraperitoneally injected for anesthesia rats for collecting brain, followed by quick-freezing at −20 °C refrigerator for 5 min. The frontal pole was cut off by a sharp blade, and the brain tissues were cut to slices every 3 mm. TTC solution (2%) was put in prevent-light cup, and then the brain slices were put into the solution for incubation for 20 min at 37 °C incubator. After staining, the slices were soaked in 4% paraformaldehyde for fixation for 10 h, followed by photographing. CI area on the same side was analyzed by the BI-2000 medical image analysis system (Olympus, Japan). The infarct volume for each piece of brain slices was product between the CI area and the thickness of CI. The total volume of infarct was the sum of the CI volume of five brain slices. The relative volume of CI = total infarct volume/contralateral brain tissue volume.

Forelimb Placement Test

After injection for 1, 7, 14, and 28 days, forelimb placed test was conducted. One side limbs of the rat were fixed on the table, and let the other side of the mobilizable forelimbs touch the edge of the table. The times of forelimbs touch the table edge in ten times were recorded. The experiment process above was repeated in the other side of limbs, and proportion of paralysis forelimbs touched table edge was calculated.

Balance Beam Walking Test

After injection for 1, 7, 14, and 28 days, motion of the model rats was tested by the balance beam walking test. All the rats were trained to adapt the balance beam for 3 days before injection until the scores of all the rats reached 6 points. The rats were placed in a wood beam about 30 cm long and 1.3 cm wide to maintain balance when it is time for observation. The evaluation standards were as follows: [12] 0 points, four limbs of rat could seize the wood surface and keep balance; 1 point, only one side of the claws could seize the wood; 2 points, 1~2 limbs slide down the wood; 3 points, three limbs slide down the wood; 4 points, the rats try to keep balance on the beam but ultimately

slide down; 5 points, rats tried to keep balance but slipped and hanging on the wood, ultimately dropped; 6 points, rats directly fall down from the beam and could not keep balance at all.

Tissue Sampling

The rats were intraperitoneally injected with 20% urethane for anesthesia. The left ventricular was rapidly infused with 100-ml saline to wash the blood vessels. After that, 200-ml glutaraldehyde (1.5%) and 200-ml paraformaldehyde (4%) were slowly injected for perfusion for 1 h. The cortical tissues between 7 and 13 nm of the top of olfactory bulb to the right side of the brain and brain sagittal split to outside 1/3 of lateral fissure were stripped.

Immunohistochemistry

The rat brain tissues were conventionally embedded by paraffin and cut into slices of 4 μm. The rabbit anti-Nestin (1: 400), NeuN (1: 400), β-III-Tub (1: 200), GFAP (1: 200), and HNA (1: 400) antibodies were purchased from Gibco company, rabbit anti-PDCD4 (1: 200) antibody was bought from Abcam company, and Biotin-sheep anti-rabbit IgG and DAB were purchased from DAKO company. Before dewaxing, the slices were placed in room temperature for 60 min, and then soaked in xylene. After being dewaxed and hydrated, the slices were added with sealing fluid and kept in room temperature for 20 min. After being added with 50 μl of primary antibody and kept in room temperature for 1 h, secondary antibody was added to the slices, followed by wash and diaminobenzidine (DAB) development. After that, the slices were dyed by hematoxylin for 2 min, and then the slices were dehydrated, cleared, sealed, and observed with the inverted microscope after differentiated by hydrochloric-alcohol solution. Five random fields of each slice were observed inverted microscope. Criteria of immunohistochemical positive are defined when brown or dark yellow particles appear in cell membrane or endochylema. The proportions of HNA, Nestin, NeuN, β-III-Tub, PDCD4, and GFAP-positive cells in all vision were counted to calculate rate of positive expression.

HE Staining

After the paraffin-embedded tissues were cut into slices, the HE staining was made respectively to observe the pathological changes of tissues by optical microscope. Then, the tissue slices were dewaxed and immersed into gradient alcohol for 10 min in each concentration and washed with running water twice in turn. Then, the slices are immersed in Harris hematoxylin liquid for 1 min and flushed with tap water for three times, then differentiated to turn the slices blue. Next, the slices are immersed in 70~80% alcohol for 1 min and in eosin solution for 1 min for coloration. Finally, the results of modeling were analyzed.

Immunofluorescence Assay

Brain tissues separated from two random rats in each group was detected by double immunofluorescence staining. Cells in S phase were labeled by 5-bromo-2-deoxyuridine (BrdU) for three consecutive days after models were established successfully for 7 days. Doublecortin (DCX) is used to label the immature neurons. BrdU was diluted to the concentration of 10 mg/ml by PBS. The rats were injected with BrdU every 2 h according to dose of 10 mg/kg for four times and were put to death 24 h after the last time of injection. Application Adobe Photoshop (version 7.0) system was used for image processing.

Western Blotting

Antigen proteins of the tissues in each group were extracted for protein quantification and SDS-PAGE. After detecting protein content, the buffer, which contained 20~50 μl protein, was sample volume; added with 5× SDS loading buffer to final concentration of 1× in 1.5 ml EP tube, and then placed in boiling water 10 min for protein denaturation. Connected power supply, voltage at 130 V for 120 min, transferred to membrane and blocked. Put polyvinylidene fluoride (PVDF) membrane into primary antibodies that Snail/E-cadherin was diluted by 5% skim milk powder/TBST overnight at 4 °C. The next day, incubated shakily at room temperature for 2 h, and the membranes were washed in TBST three times every 10 min. Placed for color development with hypersensitive ECL, then exposed in the darkroom. Besides, exposed to the developer solution 1~2 min, then to the fixer solution 1~5 min. The relative protein contents of cells in each group were obtained when the gray levels were compared between Snail/E-cadherin protein and corresponding internal reference gene β-actin by Quantity one 4.0 (Biorad Co., Ltd., USA). Each experiment was performed in triplicate.

Quantitative Real-Time Polymerase Chain Reaction

Rat brain tissues were homogenized and centrifuged at 3000 rpm for 10 min at 4 °C, and the separated supernatant was placed into a 1.5-mL EP tube, followed by numbering. The PCR kit was used to extract RNA, and RNA template (2 μg/sample) was taken for synthesis cDNA. Oligo(dT) primers 3 μl and DEPC water were added into for making a total volume of 13 μl. The mixture was pre-degenerated in 70 °C for 5 min, immediately put on ice for 5 min, and then added with 6-μl MLV buffer (5×), 2-μl dNTP, 0.5-μl RNase inhibitor, 1.5-μl MMLV reverse transcriptase, and DEPC water for making a total volume of 30 μl. The conditions for cDNA synthesis were as follows: 42 °C for 60 min, 95 °C for 10 min, and the reaction was determined, followed by preservation of cDNA at −40 °C. qRT-PCR was used to detect expressions of miR-21, PDCD4, PTEN, FasL, Nestin, β-III-Tub, GFAP, and internal reference genes (U6 and GAPDH). The primers were designed and synthesized by Shanghai Sangon Biological Engineering Co., LTD. The cDNA was added into the real-time PCR reaction system: SYBR Green Master (Rox) 10 μl (Roche, Basel, Switzerland), forward and reverse primers each 1 μl, cDNA 1 μl, DEPC water 7 μl, and the total volume of system was 20 μl. The above mixture was mixed evenly and centrifuged for conducting real-time PCR reaction. The procedures for PCR reaction was as follows: 95 °C for 30 s (pre-degeneration); 40 cycle: 95 °C for 5 s; 60 °C for 30 s, 72 °C for 20 s; finally, extension at 72 °C for 6 min. Ct value was used for results analysis and compared with the reference GAPDH using relative method. The instrument used was Real-time PCR instrument (Eppendorf, Germany). The reagents used in reverse transcription were bought from Promega (Madison, Wisconsin, USA). The primer sequences [13–15] are shown in Table 1.

DNA Laddering Assays

The tissues of each group exposed to alkaline buffer solutions 1 h (5 mM Tris–HCl pH 7.4 20 mM EDTA 0.05%Triton-X100), and then incubated in ice water 20 min. Samples were centrifuged for 20 min at 27,000 rpm. There was no DNA where there is no apoptosis in supernatant fraction since ultracentrifugation could remove DNA fragments during apoptosis. The supernatant fraction was treated with phenol/chloroform, and then nucleic acids subsided with ethanol. The samples were determined the existence of DNA laddering in 2% agarose gel electrophoresis containing ethidium bromide after hydrolyzing in 1% RNAse containing no DNAse.

TUNEL Staining

The tissues in each group were washed with xylene twice every 5 min, washed with gradient ethanol (100, 95, 90, 80, 70%) once every 3 min, respectively, and then washed with PBS twice. The tissues were treated with Proteinase K working solution for 15~30 min at 21~37 °C or added with transparent liquid for 8 min, washed with PBS twice, prepared TUNEL reaction mixture; the treatment groups mixed 50 μl TdT with 450 μl dUTP solution marked by fluorescence. Furthermore, the negative control group was added with 50 μl dUTP solution labeled by fluorescence, while the positive control group added with 100 μl DNase 1 firstly, and then reacted at room temperature about 37 °C for 10~30 min; the following step was the same with the treatment groups. After drying glass slides, the samples were added with 50-μl TUNEL reaction mixture (the negative control group was added with 50-μl dUTP solution marked by fluorescence), reacted in dark and wet box at 37 °C for 60 min using cover

Table 1 The primer sequences for quantitative real-time polymerase chain reaction (qRT-PCR)

Primer	Sequences (5′-3′)	Length (bp)
miR-21	F: CGGATCCTGGGGGTTCGATCTTAACAGGC	70
	R: CGGAATTCCCACAATGCAGCTTAGTTTTCC	
PDCD4	F: CCGCTCGAGATATAAGAACTCTTGCAGTCTTAGATG	863
	R: TCTCTCTAGAACCAGGTTCATTTTTC	
Nestin	F: TACAGCCACTGAGGTATTG	506
	R: TCACTGCCATCTGCTCATTC	
β-III-Tub	F: AGATGTACGAAGACGACGAGGAG	313
	R: GTATCCCCGAAAATATAAACACAAA	
GFAP	F: GTGGGCAGGTGGGAGCTTGATTCT	
	R: CTGGGGCGGCCTGGTATGACA	
U6	F: CTCGCTTCGGCAGCACA	300
	R: AACGCTTCACGAATTTGCGT	
GAPDH	F: TCCCCACTGCCAACGTGTCAGTG	309
	R: ACCCTGTTGCTGTAGCCAAATTCG	

F forward, *R* reverse

slips or sealing film, and washed with PBS three times. With the number of apoptotic cells counted, the percentage of cell apoptosis was calculated via one drop of PBS (the wavelength of excitation light was 450~500 nm, and the detection wavelength was 515~565 nm).

Statistical Analysis

SPSS 21.0 software was applied for data analysis; the measurement data is expressed by Mean ± SD. Comparisons on measurement data were conducted by *t* test. Intergroup difference was analyzed by applying One-way analysis of variance (ANOVA) test. $P < 0.05$ was considered statistically significant.

Results

Results of Rat Model Establishment

After 125 rats were intraperitoneally injected with alloxan, fasting blood glucose of 120 rats was ≥16.7 mmol/L. Six rats died during the production of the CI models, and the other 114 rats were successfully induced into CI models (the rate of successful modeling was 91.2%). Symptoms of the model rats included weight loss, increase of water intake, food intake and urine output, lackluster fur, high blood glucose, etc. Five rats in both the control group and the DM + CI group were randomly selected, followed by TTC staining. Normal tissues presented red and ischemic infarction area presented pale. The relative volume of CI was 54.78 ± 8.52%. Staining results were shown in Fig. 1. A total of 105 rats were randomly selected from the remaining 109 model rats and averagely divided into seven groups for the following study.

HE Staining Results of Rats in the DM + CI Group

Under light microscope, rats in the DM + CI group had obviously widened space of nerve cell surroundings in the CI area, decreased number of central neurons, and obvious hemorrhagic changes. Residual neurons also presented a series of cell necrosis situations, including nucleus pycnosis and tissue looseness (as shown in Fig. 2).

Comparisons of Forelimb Placement Experiment Results of Rats among Eight Groups

Rats were conducted with forelimb placement experiments 1 day after injection. Compared with the normal group, scores of the other seven groups significantly decreased (all $P < 0.05$), and there was no significant
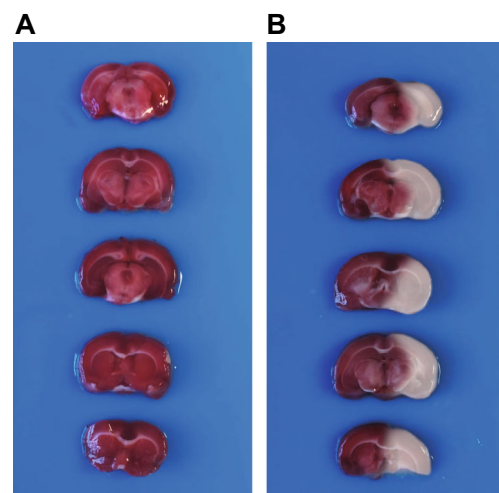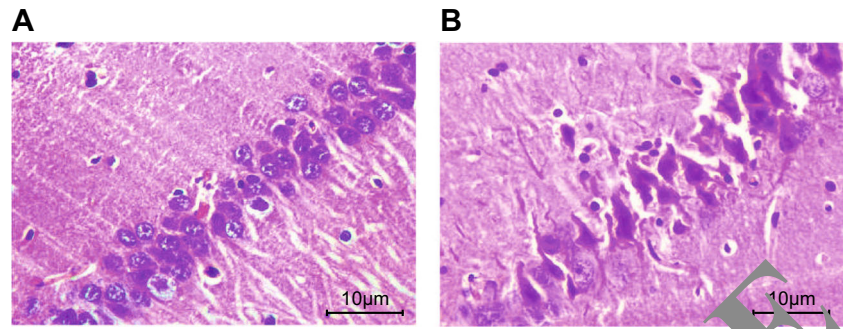

Fig. 1 Comparisons of TTC staining results between the control and DM + CI groups. Note: **a** the control group; **b** the DM + CI group. DM + CI: diabetes mellitus combined with cerebral infarction

Fig. 2 Comparisons of HE staining results between the control and DM + CI groups. Note: **a** the control group; **b** the DM + CI group. DM + CI: diabetes mellitus combined with cerebral infarction

difference was found in comparisons of scores among the other seven groups (all $P > 0.05$). In 7 days, the score of other seven groups increased significantly compared with in 1 day, except the normal group (all $P < 0.05$). Scores in the eight groups were significantly increased in comparisons between scores in 14 and 14 days, and between scores in 28 and 14 days ($P < 0.05$). Scores of rats in the blank group was significantly decreased compared with those in the normal group in 7, 14, and 28 days, respectively (all $P < 0.05$), while no such significant difference was found in comparisons between the blank group and the mimics control group, the inhibitor control group, and the miR-21 inhibitor + si-PDCD4 group ($P > 0.05$) but significantly decreased compared with the normal group ($P < 0.05$). There was no significant difference between the scores of the miR-21 mimics group and the si-PDCD4 group, which were both lower than those in the normal group and higher than those in the blank group (all $P < 0.05$). Score of miR-21 inhibitor group is significantly lower than both the normal group and the blank group (both $P < 0.05$) (as shown in Table 2).

Comparisons of the Balance Beam Walking Test Results of Rats among the Eight Groups

Rats in the normal group could keep balance in the balance beam, sprawl out on the beam, and show the desire to explore. Rats in the model group was difficult to keep balance, tried to use lateral claw to help keeping balance, and showed panic. Severe cases could not keep balance and fell off. Balance beam test scores of the rest of the seven groups in 1, 7, 14, and 28 days were significantly higher than in the normal group (all $P < 0.05$), there was no significant difference between the scores of rats in the blank group at different time points (all $P > 0.05$). In 7, 14, and 28 days, both the miR-21 mimics group and the si-PDCD4 group showed no significant differences in scores (all $P > 0.05$), but all the scores were significantly lower than in the blank group (all $P < 0.05$), while the scores of the miR-21 inhibitor group was obviously higher than in the blank group (both $P < 0.05$). In 7 days comparing with 1 day, 14 days comparing with 7 days, and 14 days comparing with 28 days, scores of rats in the miR-21 mimics and si-PDCD4 groups were significantly lower ($P < 0.05$), while the scores of rats in the miR-21 inhibitor group were increased

Table 2 Comparisons of scores of forelimb placement experiments of rats among eight groups (%)

	1 day	7 days	14 days	28 days
Normal group	99.34 ± 8.85	98.65 ± 8.32	98.08 ± 7.85	98.44 ± 8.19
Blank group	18.12 ± 3.11^d	36.61 ± 5.73^d	55.32 ± 6.36^d	66.36 ± 6.17^d
Mimics control group	20.33 ± 3.29^d	39.52 ± 7.11^d	50.52 ± 5.32^d	62.98 ± 7.58^d
miR-21 mimics group	16.99 ± 4.18^d	53.18 ± 4.99^{ade}	66.01 ± 7.98^{abde}	80.86 ± 7.13^{abcde}
Inhibitor control group	21.73 ± 4.61^d	34.75 ± 4.55^d	52.02 ± 6.52^d	68.02 ± 6.11^d
miR-21 inhibitor group	19.59 ± 3.25^d	27.55 ± 3.08^{ade}	42.69 ± 4.75^{abde}	55.06 ± 5.21^{abcde}
si-PDCD4 group	20.02 ± 3.58^d	51.01 ± 4.87^{ade}	62.98 ± 6.18^{abde}	87.02 ± 9.13^{abcde}
miR-21 inhibitor + si-PDCD4 group	22.15 ± 4.35^d	37.11 ± 4.36^d	53.72 ± 5.88^d	65.55 ± 5.52^d

[a] Compared with the same group in 1 day, $P < 0.05$

[b] Compared with the same group in 7 days, $P < 0.05$

[c] Compared with the same group in 14 d, $P < 0.05$

[d] Compared with the normal group in the same time, $P < 0.05$

[e] Compared with the blank group in the same time, $P < 0.05$

significantly ($P < 0.05$). Scores of rats in the mimics control group, the inhibitor control group, and the miR-21 inhibitor + si-PDCD4 group were significantly higher than those in the normal group at the same time points ($P < 0.05$) and had no statistical difference at the same time points compared with that in the blank group ($P > 0.05$) (Table 3).

The miR-21 Expression and the mRNA and Protein Expressions of PDCD4, HNA, Nestin, NeuN, β-III-Tub, and GFAP of Rat Brain Tissues among Eight Groups by qRT-PCR

At 28 days after injection, rats in each group were put to death and the brain tissues were separated. Immunohistochemical staining and western blotting results were shown in Fig. 3. In every model group, HNA and Nestin and PDCD4 expressions were significantly higher than those in the normal group, while NeuN, β-III-Tub, and GFAP expressions were significantly lower than those in the normal group (all $P < 0.05$). Compared with the blank group, the expressions of HNA, Nestin, and PDCD4 were significantly reduced and NeuN, β-III-Tub, and GFAP expressions were increased in the miR-21 mimics group and the si-PDCD4 group (all $P < 0.05$), while the miR-21 inhibitor group was in the opposite trend (all $P < 0.05$). No significant difference was found in the expressions of the above factors among the mimics control group, the inhibitor control group, and the miR-21 inhibitor + si-miR-PDCD4 group. Results of western blotting showed that the miR-21 mimics group and the si-PDCD4 group had lower expressions of miR-21; higher expressions of PDCD4, PTEN, and FasL; while the miR-21 inhibitor group was in the opposite trend (all $P < 0.05$). The results above indicate that

miR-21 can promote the differentiation of stem cells into nerve cells, inhibit the nerve cells apoptosis, and promote the regeneration of the nerve cells.

The miR-21 Expression and the mRNA Expressions of PDCD4, PTEN, FasL, HNA, Nestin, NeuN, β-III-Tub, and GFAP of Rat Brain Tissues among Eight Groups by Immunohistochemical Staining and Western Blotting

At 28 days after injection, the miR-21 expression and the mRNA expressions of PDCD4, PTEN, FasL, HNA, Nestin, NeuN, β-III-Tub, and GFAP in brain tissues were shown in Fig. 4. Compared with the normal group, mRNA expressions of HNA, Nestin, and PDCD4 of the blank group, the mimics control group, the inhibitor control group, the miR-21 inhibitor group, and the miR-21 inhibitor + si-PDCD4 group were significantly increased, while mRNA expressions of NeuN, β-III-Tub, GFAP, and miR-21 were significantly decreased (all $P < 0.05$). Expressions of HNA, Nestin, PDCD4, PTEN, FasL, NeuN, β-III-Tub, and GFAP and miR-21 in the miR-21 mimics group and si-PDCD4 group had no significant difference compared with those in the normal group (all $P > 0.05$). Compared with the blank group, the mRNA expression of HNA, Nestin, PTEN, FasL, and PDCD4 in the miR-21 mimics group were significantly decreased, while the mRNA expression of NeuN, β-III-Tub, GFAP, and miR-21 were increased significantly (all $P < 0.05$). The mRNA expressions of HNA, Nestin PTEN, FasL, and PDCD4 in the miR-21 inhibitor group were significantly increased, while mRNA expressions of NeuN, β-III-Tub, GFAP, and miR-21 were significantly decreased (all $P < 0.05$). The mRNA expressions of HNA, Nestin PTEN, FasL, and PDCD4 in the si-PDCD4 group were significantly decreased, while mRNA

Table 3 Comparisons of the balance beam walking test results of rats among the eight groups

	1 day	7 days	14 days	28 days
Normal group	1.03 ± 0.09	1.05 ± 0.12	1.06 ± 0.11	1.09 ± 0.13
Blank group	3.59 ± 0.23^d	3.46 ± 0.41^d	3.38 ± 0.52^d	3.44 ± 0.64^d
Mimics control group	3.64 ± 0.26^d	3.59 ± 0.19^d	3.45 ± 0.61^d	3.52 ± 0.47^d
miR-21 mimics group	3.17 ± 0.33^d	2.71 ± 0.47^{ade}	1.88 ± 0.11^{abde}	1.46 ± 0.21^{abcde}
Inhibitor control group	3.82 ± 0.42^d	3.57 ± 0.52^d	3.42 ± 0.61^d	3.51 ± 0.26^d
miR-21inhibitor group	4.15 ± 0.66^d	4.78 ± 0.55^{ade}	5.42 ± 0.37^{abde}	5.98 ± 0.38^{abcde}
si-PDCD4 group	3.08 ± 0.37^d	2.65 ± 0.59^{ade}	2.10 ± 0.29^{abde}	1.55 ± 0.17^{abcde}
miR-21 inhibitor + si-PDCD4 group	3.72 ± 0.28^d	3.62 ± 0.61^d	3.55 ± 0.16^d	3.56 ± 0.24^d

[a] Compared with the same group in 1 day, $P < 0.05$

[b] Compared with the same group in 7 days, $P < 0.05$

[c] Compared with the same group in 14 days, $P < 0.05$

[d] Compared with the normal group at the same time, $P < 0.05$

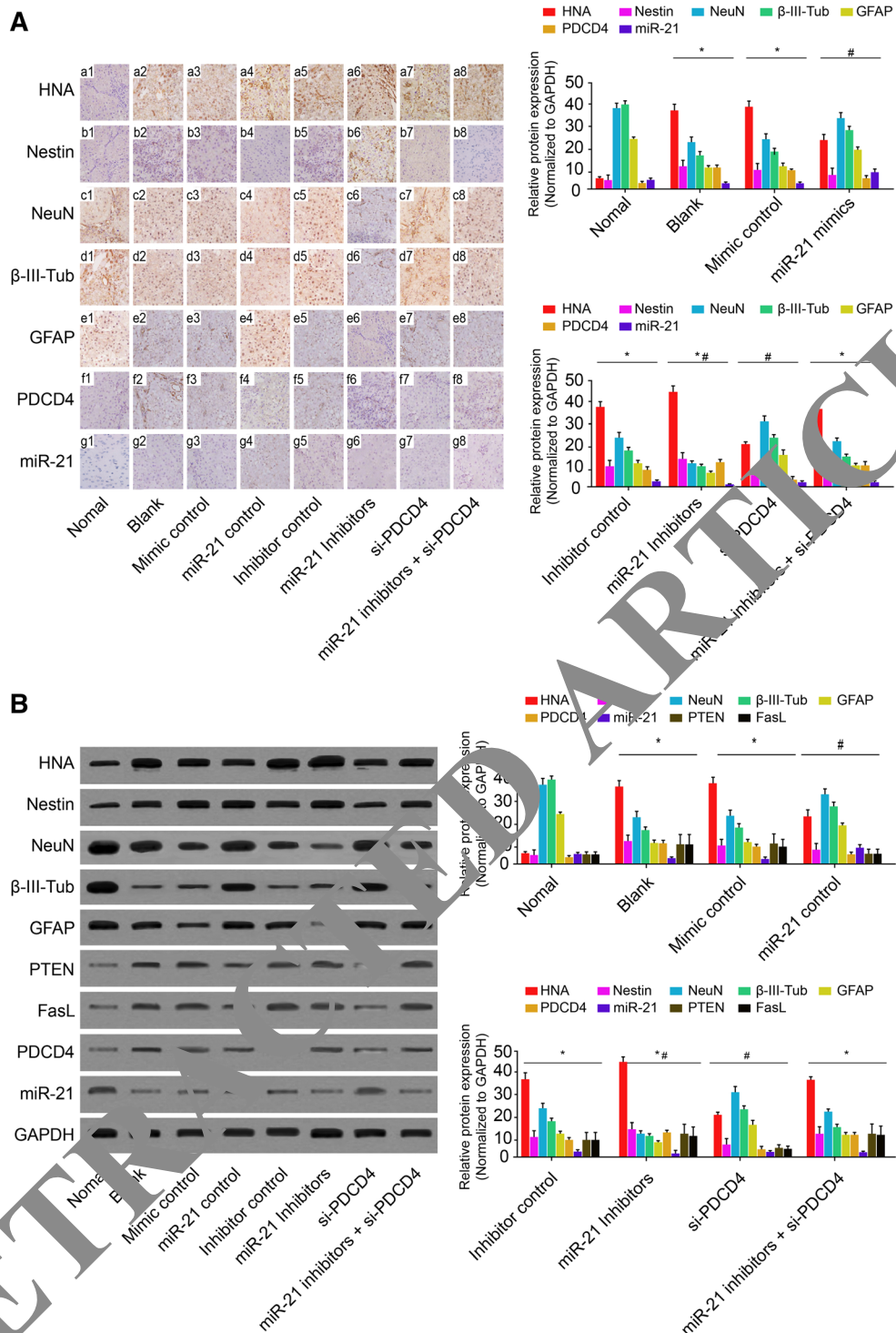[e] Comparing with the blank group at the same time, $P < 0.05$

Fig. 3 **a** The rat neural markers and the protein expressions of PDCD4, PTEN, and FasL in eight groups detected by immunohistochemical staining. Note: *Asterisk* compared with the normal group (*P* < 0.05). *number sign* compared with the blank group (*P* < 0.05). **b** The rat neural markers and the protein expressions of PDCD4, PTEN, and FasL in eight groups detected by western blotting. Note: *Asterisk* compared with the normal group (*P* < 0.05). *Number sign* compared with the blank group (*P* < 0.05)

expressions of NeuN, β-III-Tub, and GFAP were significantly increased (all *P* < 0.05), and miR-21 expression had no significant difference (*P* > 0.05). Compared with the blank group, the mRNA expressions of HNA, Nestin, NeuN, β- III-Tub, GFAP, PDCD4, PTEN, FasL, and miR-21 in the mimics control group, the inhibitor control group and the miR-21 inhibitor + si-PDCD4 group had no significant difference (all *P* > 0.05).
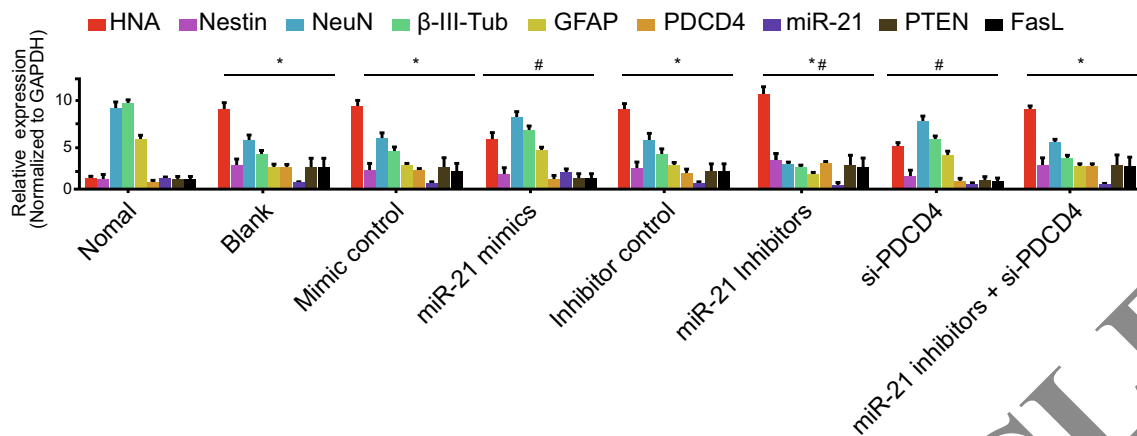
Fig. 4 The miR-21 expression and the mRNA expressions of PDCD4, PTEN, FasL, HNA, Nestin, NeuN, β-III-Tub, and GFAP of rat brain tissues among eight groups by qRT-PCR. Note: *Asterisk* compared with the normal group (*P* < 0.05). *Number sign* compared with the blank group (*P* < 0.05)

The Cell Apoptosis and DNA Damage of Nerve Cells in Eight Groups

As shown in Fig. 5, TUNEL staining and DNA laddering assays showed that the expressions of fluorescence were higher than the normal group (*P* < 0.05); compared with the blank group, expressions of fluorescence in the miR-21 mimics group and the si-PDCD4 group decreased significantly (all *P* < 0.05), and DNA laddering reduced simultaneously (all *P* < 0.05). However, the fluorescence intensity and DNA laddering in the miR-21 inhibitor group enhanced markedly in comparison to the blank group (all *P* < 0.05). The results demonstrated that overexpression of miR-21 or inhibition of PDCD4 expression can promote the regeneration of nerve cells.
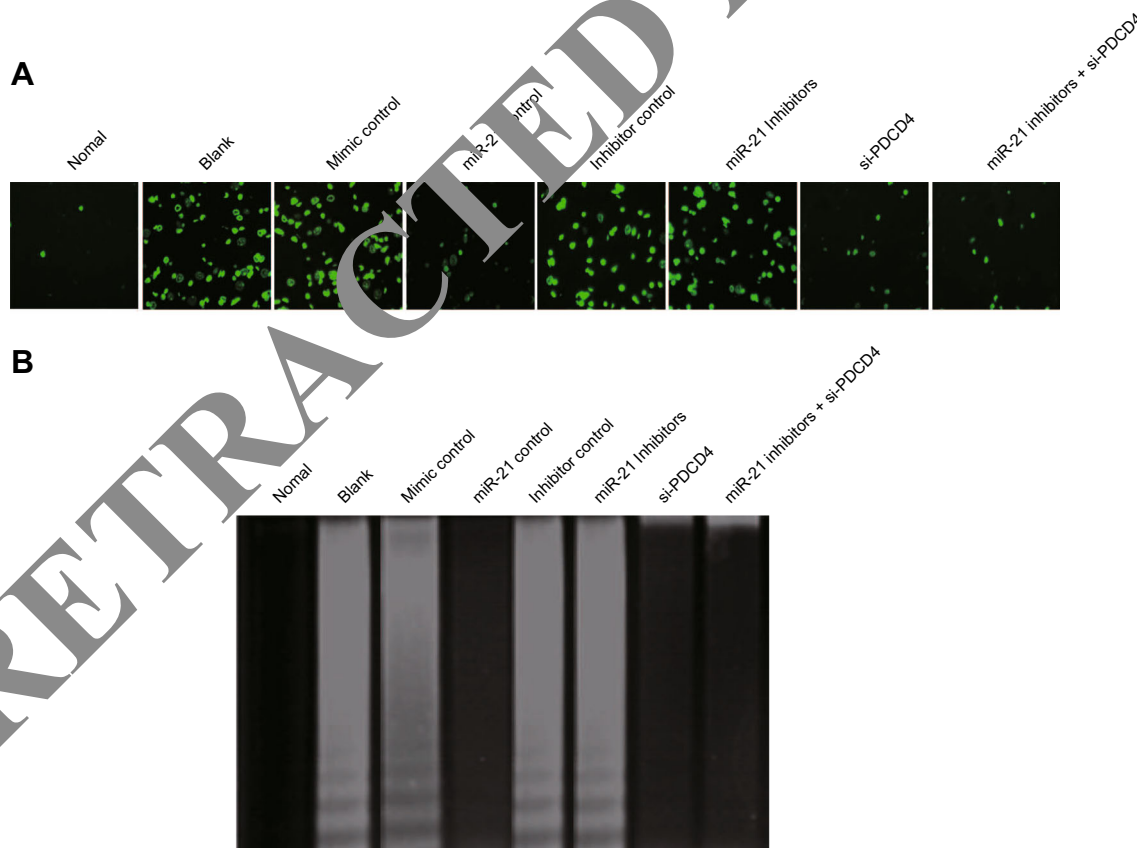

Fig. 5 a Cell apoptosis of nerve cells of rats in eight groups by TUNEL staining (×200). Note: *green fluorescent*, TUNEL positive cells; *asterisk* compared with the normal group (*P* < 0.05). *Number sign* compared with the blank group (*P* < 0.05). **b** DNA damage of nerve cells of rats in eight groups. Note: *asterisk* compared with the normal group (*P* < 0.05). *Number sign* compared with the blank group (*P* < 0.05)

The BrdU and DCX Fluorescent Expressions of Rat Brain Tissues among Eight Groups

Double immunofluorescence staining was used to detect the differences of BrdU and DCX fluorescent expressions in rat brain tissues. As shown in Fig. 6, compared with the normal group, the expression of BrdU$^+$/DCX$^+$ in the remaining seven groups were increased ($P < 0.05$). Compared with the blank group, the expression of BrdU$^+$/DCX$^+$ in the miR-21 mimics group and the si-PDCD4 group were significantly increased ($P < 0.05$). Compared with the blank group, the expression of BrdU$^+$/DCX$^+$ in the miR-21 inhibitor group decreased significantly ($P < 0.05$). The results preliminarily indicate that overexpression of miR-21 or inhibition of PDCD4 expression can promote the regeneration of nerve cells.

Discussion

Vascular complication is one of the main complications of diabetes, and cerebrovascular complications are one of the main reasons for disability and death of diabetic chronic complications [2]. The study of Wu D et al. showed that miRNAs play important an role in nerve regeneration [16]. Our present study proposed the relationship between miR-21 targeted at PDCD4 and DM + CI. The results of the experiments confirmed that exogenous overexpression of miR-21 could negatively regulate PDCD4 to promote nerve cell regeneration and improve nerve defect status of DM + CI rats, which promote the recovery of neural function.
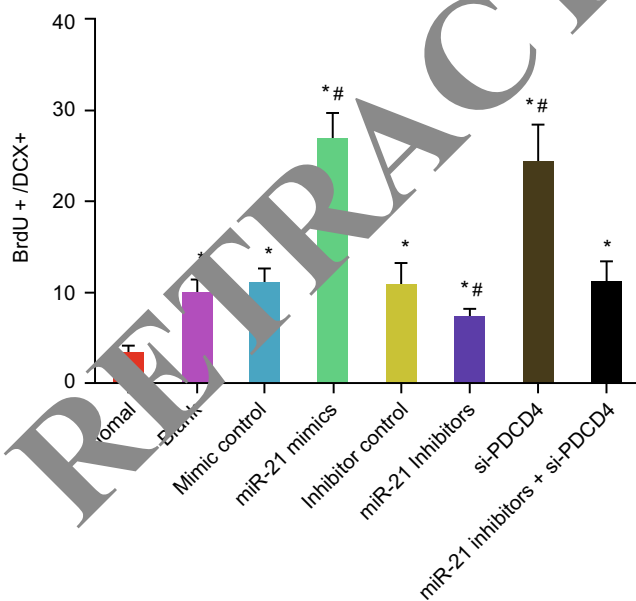

Fig. 6 Results of BrdU and DCX fluorescent expressions of rat brain tissues among eight groups. Note: *Asterisk* compared with the normal group ($P < 0.05$). *Number sign* compared with the blank group ($P < 0.05$)

Many previous studies have confirmed that PDCD4 is the direct target gene of miR-21, and PDCD4 was negatively regulated by miR-21 [17–20]. PDCD4 is a tumor-suppressor gene associated with cell cycle and apoptosis, which can combine with the initial translation factor in eukaryotic cells, factor translation eukaryotic initiation factor-4A (eIF4A), to inhibit the formation of the ribosome complex and protein synthesis, which lead to cell apoptosis [21]. PDCD4 inhibits activity of nuclear transcription factor activatorprotm-1 (AP-1) to inhibit tumor growth [22]. Inhibition of PDCD4, whose downregulation will release its inhibition on protein kinase B (PKB), results in significantly reduced apoptosis in cancer cells [23]. A previous study by Poyil Pratheeshkumar et al. showed that miR-21 combines with 3′UTR of target gene PDCD4 to inhibit expression of PDCD4 in cells [11]. Furthermore, a previous study also showed that in gastric cancer tissues, miR-21 was highly expressed, and negatively correlated with PDCD4, but was almost completely inhibited after transfection of miR-21 inhibitor and, at the same time, PDCD4 expression increased [24]. On the other hand, Mao XH et al. found that inhibition of miR-21 expression can induce the expression of target proteins such as PTEN, PDCD4 to inhibit the cell proliferation and migration [25]. These previous studies indicate that miR-21 plays a crucial role in cell growth, proliferation, and apoptosis.

In this study, it was found that overexpression of miR-21 could reduce PDCD4 and promote nerve cell regeneration, improve nerve defect status of DM + CI rats, and thus promote the recovery of neural function. The expression of miR-21 is usually detected in some malignant tumors, such as prostate cancer, colorectal cancer, lung cancer, pancreatic cancer, etc. [26–28]. The study of Ni et al. suggests that miR-21 expression was increased during the differentiation of neural crest stem cells [29]. Previous study confirmed that overexpression of miR-21 promotes the regeneration of neural cells [30]. The studies mentioned above suggest miR-21 plays an important role in regulating growth pathways following peripheral nerve injury. Moreover, reduction of apoptosis-correlated gene PDCD4 can inhibit the occurrence of apoptosis and protect the cells [31]. ZHU et al. found that the expression of miR-21 was inversely correlated with the protein expression of a previously identified target gene, PDCD4, and the inhibition of miR-21 suppressed cell migration and invasion by upregulating expression of PDCD4 [32]. Furthermore, Ahmed et al. also demonstrated that selected BMP-dependent tumor-suppressor genes such as PDCD4, etc. could be negatively regulated by miR-21 [33]. The above studies suggest that miR-21 protects cells by inhibiting the expression of PDCD4 in a variety damage models. It can be inferred that exogenous overexpression of miR-21 promotes the regeneration of rat neural cells and recovery of neurological function after injury of DM + CI.

In order to further verify the recovery of rat neural function, sensitivity experiments including forelimb placement test and the balance beam walking test were used. The results showed that miR-21 mimics and si-PCDC4 improved the nerve defect of model rats, significantly raised the score of forelimb placement test, reduced the balance beam walking test score, and significantly improved the nerve defect status. This study suggests that exogenous overexpression of miR-21 improves sensorimotor function recovery after DM + CI.

Taken together, this study provided evidence that miR-21 could promote the nerve cell regeneration, inhibit the nerve cell apoptosis, and improve the nerve defect situation of DM + CI rats by inhibiting PDCD4. Its mechanism may be related to that overexpression of miR-21 inhibits the expression of PDCD4. This study provided new theoretical evidences for miR-21 molecular target therapy for DM + CI in clinic. However, nerve cell regeneration and neural functional recovery of DM + CI rats may be a result of multipoint control of multiple miRNAs and multiple target genes. Furthermore, due to the limitation of finance and time, we cannot repeat the experiment in the CI rat model. And, the specific mechanism remains to be further researched.

Compliance with Ethical Standards

Conflict of Interests The authors declare that they have no competing interests.

References

1. Okwechime IO, Roberson S, Odoi A (2015) Prevalence and predictors of pre-diabetes and diabetes among adults 18 years or older in Florida: a multinomial logistic modeling approach. PLoS One 10(12):e0145781

2. Ashcroft FM, Rorsman P (2012) Diabetes mellitus and the beta cell: the last ten years. Cell 148(6):1160–1171

3. Mingrone G, Panunzi S, De Gaetano A, Guidone C, Iaconelli A, Leccesi L, Nanni G, Pomp A et al (2012) Bariatric surgery versus conventional medical therapy for type 2 diabetes. N Engl J Med 366(17):1577–1585

4. Janna S, Bhowmik NB, Alam D (2015) Clinical profile of ischemic stroke in type 2 diabetic patients: experience in a tertiary care hospital [J]. Eastern Medical Journal 5(2):88–91

5. Bellacqua M, Dominguez LJ, Barrella M, Barbagallo M (2007) Induction of vascular endothelial growth factor release by transcutaneous frequency modulated neural stimulation in diabetic polyneuropathy. J Endocrinol Investig 30(11):944–947

6. Higashi Y (2009) Edaravone for the treatment of acute cerebral infarction: role of endothelium-derived nitric oxide and oxidative stress. Expert Opin Pharmacother 10(2):323–331

7. Liu G, Friggeri A, Yang Y, Milosevic J, Ding Q, Thannickal VJ, Kaminski N, Abraham E (2010) miR-21 mediates fibrogenic activation of pulmonary fibroblasts and lung fibrosis. J Exp Med 207(8):1589–1597

8. Hu A, Huang JJ, Xu WH, Jin XJ, Li JP, Tang YJ, Huang XF, Cui HJ et al (2014) miR-21 and miR-375 microRNAs as candidate diagnostic biomarkers in squamous cell carcinoma of the larynx: association with patient survival. Am J Transl Res 6(5):604–613

9. Cheng Y, Zhu P, Yang J, Liu X, Dong S, Wang X, Chun B, Zhuang J et al (2010) Ischaemic preconditioning-regulated miR-21 protects heart against ischaemia/reperfusion injury via anti-apoptosis through its target PDCD4. Cardiovasc Res 87(3):431–439

10. Pratheeshkumar, P., Y.O. Son, S.P. Divya, L. Wang, L. Turcios, R.V. Roy, J.A. Hitron, D. Kim, J. Dai, P. Asha, Z. Zhang, and X. Shi (2016) Quercetin inhibits Cr(VI)-induced malignant cell transformation by targeting miR-21-PDCD4 signaling pathway. Oncotarget

11. Pratheeshkumar, P., Y.O. Son, S.P. Divya, L. Turcios, R. Roy, J.A. Hitron, L. Wang, D. Kim, J. Dai, P. Asha, Z. Zhang, and X. Shi (2016) Hexavalent chromium induces malignant transformation of human lung bronchial epithelial cells via ROS-dependent activation of miR-21-PDCD4 signaling. Oncotarget

12. Feeney DM, Gonzalez A, Law WA (1982) Amphetamine, haloperidol, and experience interact to affect rate of recovery after motor cortex injury. Science 217(4562):855–857

13. Kapoor I, Kanaujiya J, Kumar Y, Thota JR, Bhatt ML, Chattopadhyay N, Sanyal S, Trivedi AK (2016) Proteomic discovery of MNT as a novel interacting partner of E3 ubiquitin ligase E6AP and a key mediator of myeloid differentiation. Oncotarget 7(7):7640–7656

14. Charkiewicz R, Pilz L, Sulewska A, Kozlowski M, Niklinska W, Moniuszko M, Reszec J, Manegold C et al (2016) Validation for histology-driven diagnosis in non-small cell lung cancer using hsa-miR-205 and hsa-miR-21 expression by two different normalization strategies. Int J Cancer 138(3):689–697

15. Steffensen R, Baech J, Nielsen KR (2015) Allelic discrimination by TaqMan-PCR for genotyping of human neutrophil antigens. Methods Mol Biol 1310:205–212

16. Wu D, Raafat A, Pak E, Clemens S, Murashov AK (2012) Dicer-microRNA pathway is critical for peripheral nerve regeneration and functional recovery in vivo and regenerative axonogenesis in vitro. Exp Neurol 233(1):555–565

17. Asangani IA, Rasheed SA, Nikolova DA, Leupold JH, Colburn NH, Post S, Allgayer H (2008) MicroRNA-21 (miR-21) post-transcriptionally downregulates tumor suppressor Pdcd4 and stimulates invasion, intravasation and metastasis in colorectal cancer. Oncogene 27(15):2128–2136

18. Sheedy FJ, Palsson-McDermott E, Hennessy EJ, Martin C, O'Leary JJ, Ruan Q, Johnson DS, Chen Y et al (2010) Negative regulation of TLR4 via targeting of the proinflammatory tumor suppressor PDCD4 by the microRNA miR-21. Nat Immunol 11(2):141–147

19. Motoyama K, Inoue H, Mimori K, Tanaka F, Kojima K, Uetake H, Sugihara K, Mori M (2010) Clinicopathological and prognostic significance of PDCD4 and microRNA-21 in human gastric cancer. Int J Oncol 36(5):1089–1095

20. Najafi Z, Sharifi M, Javadi G (2015) Degradation of miR-21 induces apoptosis and inhibits cell proliferation in human hepatocellular carcinoma. Cancer Gene Ther 22(11):530–535

21. Waters LC, Strong SL, Ferlemann E, Oka O, Muskett FW, Veverka V, Banerjee S, Schmedt T et al (2011) Structure of the tandem MA-3 region of Pdcd4 protein and characterization of its interactions with eIF4A and eIF4G: molecular mechanisms of a tumor suppressor. J Biol Chem 286(19):17270–17280

22. Wang Q, Zhang Y, Yang HS (2012) Pdcd4 knockdown up-regulates MAP4K1 expression and activation of AP-1 dependent transcription through c-Myc. Biochim Biophys Acta 1823(10):1807–1814

23. Liu G, Keeler BE, Zhukareva V, Houle JD (2010) Cycling exercise affects the expression of apoptosis-associated microRNAs after spinal cord injury in rats. Exp Neurol 226(1):200–206

24. Yin, K., M. Liu, M. Zhang, F. Wang, M. Fen, Z. Liu, Y. Yuan, S. Gao, L. Yang, W. Zhang, J. Zhang, B. Guo, J. Xu, H. Liang, X.

Chen, and W. Guan (2016) miR-208a-3p suppresses cell apoptosis by targeting PDCD4 in gastric cancer. Oncotarget

25. Mao, X.H., M. Chen, Y. Wang, P.G. Cui, S.B. Liu, and Z.Y. Xu (2016) MicroRNA-21 regulates the ERK/NF-kappaB signaling pathway to affect the proliferation, migration, and apoptosis of human melanoma A375 cells by targeting SPRY1, PDCD4, and PTEN. Mol Carcinog

26. Bonci D, De Maria R (2016) miR-15/miR-16 loss, miR-21 upregulation, or deregulation of their target genes predicts poor prognosis in prostate cancer patients. Mol Cell Oncol 3(4):e1109744

27. Li, C., L. Song, Z. Zhang, X.X. Bai, M.F. Cui, and L.J. Ma (2016) MicroRNA-21 promotes TGF-beta1-induced epithelial-mesenchymal transition in gastric cancer through up-regulating PTEN expression. Oncotarget

28. Lasithiotaki, I., E. Tsitoura, A. Koutsopoulos, E. Lagoudaki, C. Koutoulaki, G. Pitsidianakis, D.A. Spandidos, N.M. Siafakas, G. Sourvinos, and K.M. Antoniou (2016) Aberrant expression of miR-21, miR-376c and miR-145 and their target host genes in Merkel cell polyomavirus-positive non-small cell lung cancer. Oncotarget

29. Ni Y, Zhang K, Liu X, Yang T, Wang B, Fu L, A L, Zhou Y (2014) miR-21 promotes the differentiation of hair follicle-derived neural crest stem cells into Schwann cells. Neural Regen Res 9(8):828–836

30. Strickland IT, Richards L, Holmes FE, Wynick D, Uney JB, Wong LF (2011) Axotomy-induced miR-21 promotes axon growth in adult dorsal root ganglion neurons. PLoS One 6(8):e23423

31. Zhao, Y. and Z. Ma (2016) Swimming training affects apoptosis-related microRNAs and reduces cardiac apoptosis in mice. Gen Physiol Biophys

32. Zhu Q, Wang Z, Hu Y, Li J, Li X, Zhou L, Huang Y (2012) miR-21 promotes migration and invasion by the miR-21-PDCD4-AP1 feedback loop in human hepatocellular carcinoma. Oncol Rep 27(5):1660–1668

33. Ahmed MI, Mardaryev AN, Lewis CJ, Sharov AA, Botchkareva NV (2011) MicroRNA-21 is an important downstream component of BMP signalling in epidermal keratinocytes. J Cell Sci 124(Pt 20): 3399–3404